A new physical barrier system for seawater intrusion control

Antoifi Abdoulhalik, School of Natural and Built Environment, Queen's University Belfast, David Keir Building, Stranmillis Road, Belfast, BT95AG, UK

Ashraf Ahmed, School of Natural and Built Environment, Queen's University Belfast, David Keir Building, Stranmillis Road, Belfast, BT95AG, UK

G.A. Hamill, School of Natural and Built Environment, Queen's University Belfast, David Keir Building, Stranmillis Road, Belfast, BT95AG, UK

Corresponding author: Ashraf Ahmed (a.ahmed@qub.ac.uk)

ABSTRACT

The construction of subsurface physical barriers is one of various methods used to control seawater intrusion (SWI) in coastal aquifers. This study proposes the mixed physical barrier (MPB) as a new barrier system for seawater intrusion control, which combines an impermeable cutoff wall and a semi-permeable subsurface dam. The effect of the traditionally-used physical barriers on transient saltwater wedge dynamics was first explored for various hydraulic gradients, and the workability of the MPB was thereafter thoroughly analysed. A newly developed automated image analysis based on light-concentration conversion was used in the experiments, which were completed in a porous media tank. The numerical code SEAWAT was used to assess the consistency of the experimental data and examine the sensitivity of the performance of the barriers to various key parameters. The results show that the MPB induced a visible lifting of the dense saline flux upward towards the outlet by the light freshwater. This saltwater lifting mechanism, observed for the first time, induced significant reduction to the saline water intrusion length. The use of the MPB yielded up to 62% and 42% more reduction of the saltwater intrusion length than the semi-permeable dam and the cutoff wall, respectively. The performance achieved by the MPB with a wall depth of 40% of the aquifer thickness was greater than that of a single cutoff wall with a penetration depth of 90% of the aquifer thickness (about 13% extra reduction). This means that the MPB could produce better seawater intrusion reduction than the traditionally used barriers at even lower cost.

Keywords: Physical barriers; Saltwater intrusion mitigation; Salinization; Management of coastal aquifers.

1. Introduction

Seawater intrusion (SWI) has occurred in many coastal regions around the world (Bear et al., 1999). With the rise of sea levels and uncontrolled freshwater extraction from coastal regions, saltwater may advance further inland and contaminate the available groundwater supply (Oude Essink, 2001; Fergusson and Glesson, 2012). For water resources managers, today's challenge is to establish effective measures to control SWI and enable an optimal exploitation of groundwater resources. Previous studies in the literature have proposed several countermeasures to prevent or mitigate SWI; among these has been the installation of subsurface barriers, which can be of hydraulic or physical nature (Abarca, 2006; Oude Essink, 2001).

Hydraulic barriers can be divided into three types: positive, negative, and mixed barriers. In positive barriers (Fig 1a), freshwater is injected into the aquifer to raise the water table, which impedes the inland motion of the saltwater. The water is often injected through recharge wells installed in series along the coastline to create a freshwater ridge. Although the effectiveness of positive barriers has been argued in some studies (Abarca et al., 2006), recent studies have shown that an effective saltwater repulsion could only be achieved if the water is injected at the toe of the saltwater wedge (Botero-Acosta and Donado, 2015; Luyun et al., 2011). This highlights a significant limitation of positive barriers, considering that the saltwater wedge is never completely stationary in real-world scenarios but moves back and forth with seasonal oscillations (Luyun et al., 2009).

Negative barriers (Fig 1b) involve the interception of the intruding saltwater by pumping near the coast. Although the landward motion of the saltwater could be slowed, it was found that these barriers extract more freshwater than saltwater which eventually leads to a decrease of the available groundwater resources (Pool and Carrera, 2010). In addition, this method is only effective if the saltwater abstraction rate exceeds the freshwater pumping rate, thus involving a considerable and continuous amount of energy (Sriapai et al., 2012). The disposal of the abstracted saline groundwater could also be a source of concern (Kumar, 2006). A mixed hydraulic barrier (Fig 1c) combines a positive barrier and a negative barrier. Freshwater is injected inland to repulse the saltwater wedge, while saltwater is extracted near the shore to slow its encroachment (Basdurak et al., 2007; Pool and Carrera, 2010). In addition to the limitations mentioned above, this measure would require significant operational and maintenance costs due to the high risk of clogging and reduction of filtering area of the screen generally involved in the use of wells (Bear, 1979).

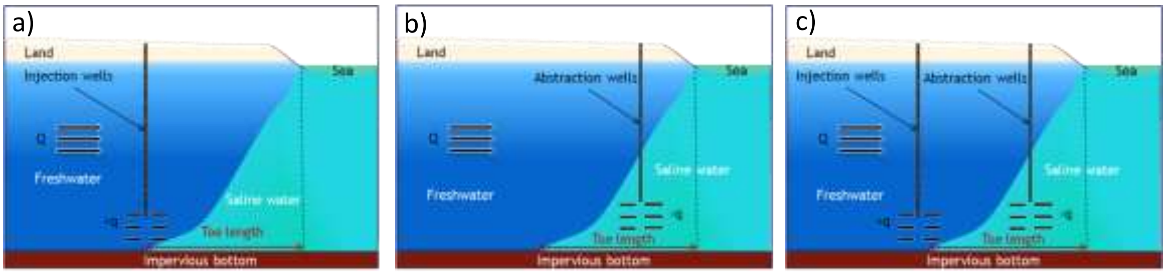

Figure 1 Simplified diagrams showing the various hydraulic barriers; a) Positive barrier, b) Negative barrier and c) Mixed hydraulic barrier.

The use of physical barriers as a SWI control method has been the focus of several studies (Archwichai et al., 2005; Sugio et al., 1987; Mundzir, 2001; Anwar, 1983; Kaleris and Ziogas, 2013; Luyun et al., 2009, 2011; Strack, 2016) . Physical barriers are subsurface impermeable or semi-permeable structures constructed parallel to the coast. Two types of physical barriers are described in the literature: the subsurface dams and the cutoff walls. The subsurface dam is embedded at the impervious bottom layer of the aquifer and obstructs its lower part only, leaving an opening above it to allow the natural discharge of freshwater to the ocean. This method has met great success in Japan, where seven out of fifteen subsurface dams were specifically designed to prevent landward incursion of saltwater and preserve fresh groundwater storage (Luyun et al., 2009; Japan Green Resources Agency, 2004). In Luyun et al. (2009), it was demonstrated that subsurface dams with smaller height could achieve faster removal of inland residual saltwater as well as more reduction of the expected increase of the saltwater wedge height along the coastline boundary than higher dams. The dam height only needs to exceed the height of the saltwater wedge at the desired construction location.

The second type of physical barrier is cutoff walls, which extend from the top of the aquifer to a predefined depth. The effectiveness of cutoff walls increases when they are closer to the coastline and have greater penetration depth (Luyun et al., 2011). The closer the cutoff wall is installed to the coast, the larger the fresh groundwater volume would be. Kaleris and Ziogas (2013) found that the performance of cutoff walls located at distances from the coastline of the order of half of the aquifer height depends not only on the penetration depth, but also on the ratio of the groundwater inflow velocity over the density driven saltwater velocity.

Controlling the velocity ratio would not only better help to repulse saltwater intrusion, but it would also allow an increased freshwater storage for a more optimal exploitation of the available freshwater resource. This concept of combined actions on saltwater intrusion has never been applied to physical barriers before. To address this point, this paper proposes the mixed physical barrier (MPB), which combines an impermeable cutoff wall located close to the shore, and a short semi-permeable subsurface dam placed at the seaward side of the cutoff wall. The aim of the new MPB system is to increase the velocity ratio, and hence further enhance the capability of repulsing the seawater wedge.

The main objectives of this study are therefore 1) to investigate the effect of semi-permeable dams and cutoff walls on transient saltwater intrusion dynamics and 2) to assess the viability of MPB as a new SWI control method. To the best of our knowledge, these objectives have never been investigated in previous studies. Experimental automated image analysis technique (Robinson et al., 2015) was used here to quantify the main SWI parameters. The methodology allowed quantitative analysis of the effect of the barriers on the toe length under transient conditions with high spatial and temporal resolution. The numerical model SEAWAT was used to assess the consistency of the experimental results with the numerical predictions. A sensitivity analysis was then performed to evaluate the dependency of the effectiveness of each barrier on some key design variables.

2. Experimental approach

2.1 Description of the experimental set-up

The experiments were completed in a flow tank of dimension 0.38 x 0.15 x 0.01 m (Fig 2). The narrowness of the tank enabled the simulation of a two dimensional system representing a cross section of an unconfined coastal aquifer. The tank was composed of a porous media chamber and two side reservoirs. The porous media chamber was filled with glass beads of mean diameter 1.1 mm. The beads were packed under saturated conditions to avoid risk of air entrapment. The beads were packed in three layers of similar thickness and each layer was carefully compacted. The resulting porous domain was assumed to satisfy homogeneous isotropic conditions. Two fine mesh acrylic screens were used to separate the porous media chamber from the side reservoirs.

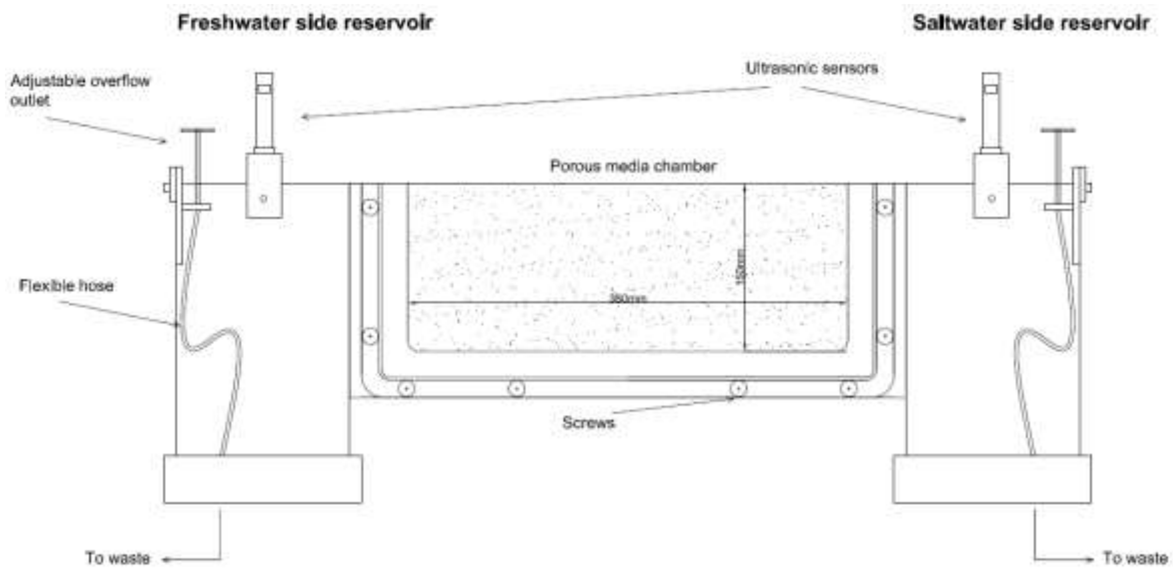

Figure 2 Schematic diagram of the porous media tank

The left side reservoir was used to feed freshwater flow to the system, and the right side reservoir was filled with saltwater. The hydraulic conductivity of the system was measured in situ using similar methods described in Oostrom et al. (1992) without considering the capillary fringe. The average hydraulic conductivity value of the porous media was estimated at 0.014

m/s. A 200*l* saltwater solution was prepared prior the experiments by dissolving commercial salt into freshwater at a concentration of 36.16 *g/l* to achieve a density of 1025 kg/m^3. The density was measured using a hydrometer (H-B Durac plain-form holycarbonate) and also manually using mass/volume ratio. To distinguish the saltwater from the freshwater, red dye (food colour) was added to the saltwater solution at a concentration of 0.15 g/*l*. In all the experiments, the saltwater solution was sourced from the 200*l* batch to ensure uniformity of density and colour between the experiments.

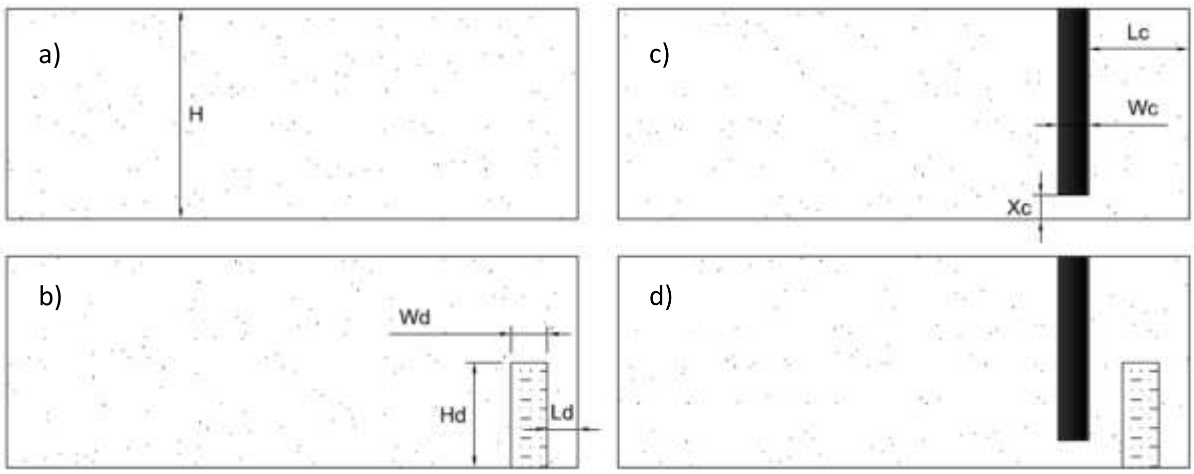

Figure 3 Investigated cases: a) baseline case; b) subsurface dam case; c) cutoff wall case; d) MPB case. The freshwater flows from left to right.

Fig 3 presents the various experimental cases investigated herein. The height of the synthetic aquifer (saturated thickness) was H=136 mm in all the experiments. The barriers were placed ahead of the packing of the beads. To form the semi-permeable dam, two dividers were inserted into the porous media chamber at the desired location, and fine beads of mean diameter 0.3 mm were siphoned into the spacing between them until the desired height. On completion of the packing, the dividers were carefully removed. The average hydraulic conductivity of the dam was also obtained by in situ measurement on the experimental flow tank (using finer mesh screens on both sides) and was found K_d = 0.0017 m/s. In field applications, typical grouting materials include soil–cement–bentonite that could exhibit hydraulic conductivities as low as 10^{-9} m/s are used (Kaleris and Ziogas, 2013).

The cutoff wall was made of impermeable material (plasticine). Cutoff walls are generally located at distances from the coastline less than or equal to twice the aquifer height (Allow, 2012; Japan Green Resources Agency, 2004) and should be located within the area of the saltwater wedge to be effective (Luyun et al., 2011). To meet these conditions, the cutoff wall was placed at a distance in the order of half of the aquifer height in our investigations. It was ensured that the cutoff wall was located within the saltwater wedge area by first analysing the saltwater wedge extent in a synthetic aquifer free of barrier (base case), as described below. The cutoff wall depth was adjusted such that an opening smaller than 40% of the aquifer height from the bottom of the tank was left to ensure effective reduction of the saltwater intrusion length (Kaleris and Ziogas, 2013). Note that the maximum wall depth of construction applicable in real field aquifers is up to 100 m (Kaleris and Ziogas, 2013). Table 1 presents a summary of the dimensions and location of the dam and cutoff wall barriers. For the MPB experiment, the cutoff wall and the semi-permeable dam were both placed in same positions as in the other experiments.

Table 1 Values of the design variables

Variable	Symbol	Values
Subsurface dam		
Distance from seawater boundary	L_d	20 mm
Height	H_d	70 mm
Width	W_d	24 mm
Hydraulic conductivity	K_d	0.0017 m/s
Cutoff wall		
Distance from seawater boundary	L_c	66 mm
Opening	X_c	16 mm
Width	W_c	20 mm

2.2 Experimental procedure

All the experiments were recorded using a high speed camera (IDT Motion Pro X – series). Prior to each experiment, a calibration method was implemented to correlate the light intensity of the recorded images to the salt concentration. The calibration method included the flushing of the domain with saltwater solutions at various concentrations, and the light intensity of every concentration for every single pixel was recorded, as detailed in Robinson et al. (2015). A MATLAB code was used to obtain the intensity-concentration parameters and then analyse all the experimental images. The light intensity-concentration conversion allowed the determination of key SWI intrusion parameters under transient conditions.

At the start of each experiment, freshwater was injected at constant rate from a large tank located above the left side reservoir and the freshwater level was set high enough to allow the entire porous media to remain fully saturated with freshwater. Freshwater flux transited through the system from the inland boundary and exited at the coastal boundary without overflowing. On the saltwater reservoir, the overflow outlet was adjusted to maintain a constant head of 129.7 mm. Excess amount of saltwater was supplied from another large tank into the right reservoir to ensure the flushing out of any freshwater floating at the surface, until the density measurement became stable. Ultrasonic sensors (Microsonic - mic+25/DIU/TC) were used to monitor all the head values with +/- 0.2mm accuracy.

The simulation of groundwater fluctuations was achieved by varying the freshwater level. For each experiment, two different heads were successively forced at the freshwater boundary, namely 135.7mm and 133.7mm, yielding a head differences of *dh*=6mm (135.7-129.7) and *dh*=4 mm (133.7-129.7), each for 50 minutes to allow the system to reach a quasi-steady state condition. The head differences *dh*=6mm and *dh*=4mm corresponded to hydraulic gradients of 0.0158 and 0.0105, respectively, which is consistent with previous laboratory studies using similar experimental set up (Robinson et al, 2015, 2016; Goswami and Clement, 2007; Chang and Clement, 2012) and within the range of hydraulic gradient measured at some field sites (e.g. Ferguson and Gleesson, 2012; Attanayake and Michael, 2007). The initial condition was set by forcing a head of 135.7 mm at the freshwater boundary (*dh*=6mm). The denser saltwater was allowed to intrude into a fully fresh aquifer, until the system reached the first quasi-steady state condition. The freshwater level was then decreased to 133.7 mm (*dh*=4mm), allowing the saltwater wedge to migrate further inland. The freshwater head was then returned to the initial value of *dh*=6 mm, which forced the saltwater wedge to recede toward the seawater boundary. The use of the same head difference *dh*=6mm as that used to set the initial condition was also to check if any hysteresis occurs over the course of the experiment.

To assess the effectiveness of the different barriers, a baseline case with no barrier installed was first studied to be used as a benchmark for the barrier cases investigated. The effectiveness of the barriers was characterised by the percentage of reduction $R = (TL_0 - TL_b)/TL_0$, where TL_0 and TL_b are the intrusion length before and after the installation of the barrier, respectively.

3. Description of the numerical model and procedure

The MODFLOW family variable density flow code SEAWAT (Guo and Langevin, 2002) has been widely used to solve various variable density benchmark problems (Goswami and Clement, 2007; Johannsen et al., 2002; Chang and Clement, 2012, 2013), including saltwater experiments involving freshwater head boundary variations. The domain was evenly discretised with a grid size of 0.2 cm. The longitudinal dispersivity was estimated after trial and error process and was eventually estimated at 0.1 cm and the transverse dispersivity was 0.05 cm, which is within the range of dispersivity values reported in Abarca and Clement (2009).The spatial discretization satisfies the criterion of numerical stability, i.e. grid Peclet number is less or equal to four (Voss and Souza, 1987). The molecular diffusion was neglected in all the numerical experiments. The specific storage was set at 10^{-6} cm^{-1}. Densities of the freshwater and saltwater were 1000 kg/m^3 and 1025 kg/m^3, respectively. A concentration of 36.16 *g/l* was used for the seawater boundary, corresponding to the amount of salt required to prepare the saltwater solution.

To simulate the transient saltwater intrusion, three stress periods were applied. Each stress period lasted 50 minutes, which corresponds to the duration required for the system to reach approximate steady state condition observed in the physical model. The time step was set to 30 sec. A variable-head boundary condition was set on the freshwater side (C=0 g/l), where it varied from 135.7 to 133.7 mm, and a constant-head of 129.7 mm was set on the saltwater side (C=36.16 g/l). The initial condition of the numerical model corresponded to a fully freshwater aquifer. The boundary conditions were forced on both sides and the system was allowed to reach the first quasi-steady state condition. The head and concentration resulting in each cell at the end of each stress period were used as initial condition for the following transient period. The subsurface dam was simulated into the numerical model by assigning the hydraulic conductivity K_d = 0.0017 m/s to the cells of interest, which correspond to the value measured in the setup, while the cutoff wall was assumed to be impermeable.

4. Results and discussion

4.1 Baseline case

In the following discussion, the toe length (*TL*) refers to the distance that the 50% saltwater concentration isoline has penetrated the aquifer from the coastal boundary. Moreover, a steady state here does not refer to complete steady state as defined in fluids flow; it refers to quasi-steady state where the wedge becomes stable with no further intrusion or retreat albeit very slight forward/backward movement may happen due to tiny boundary head fluctuations and this will be shown in the figures.

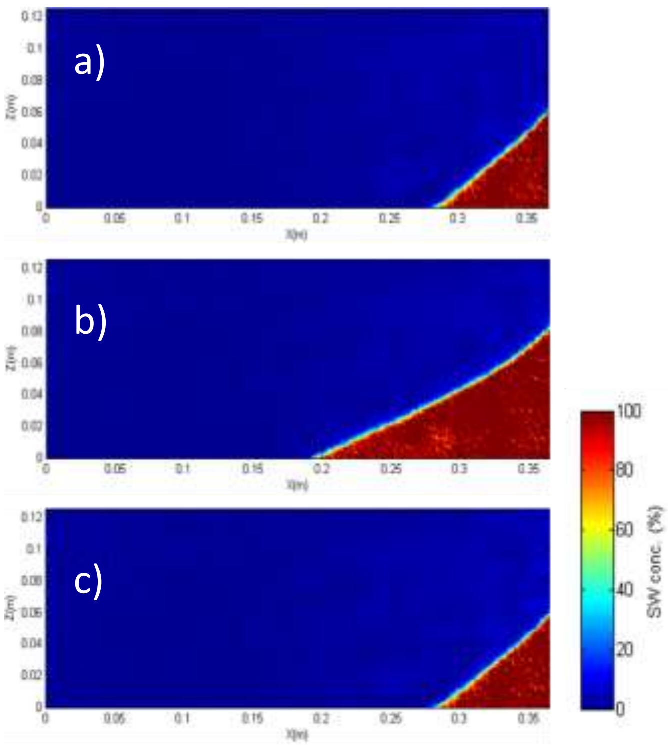

Figure 4 Steady-state experimental saltwater wedge in the base case; a) t = 0 min (initial condition); b) at t = 50 min (*dh*=4mm); c) at t = 100 min (*dh*=6mm)

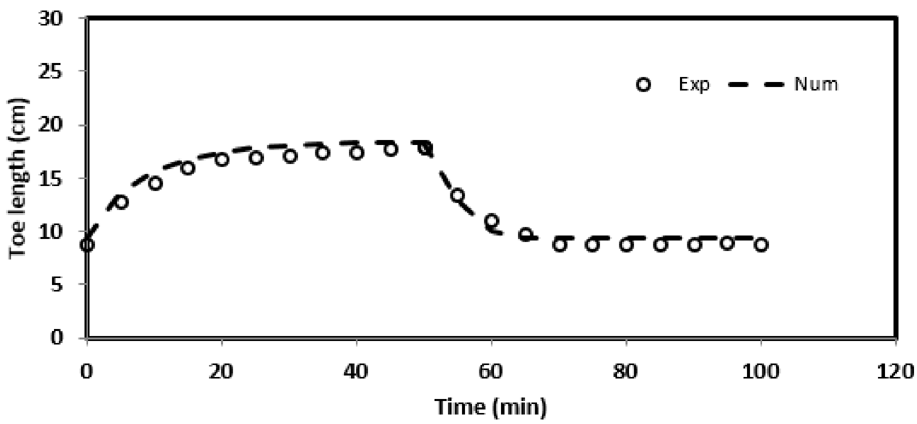

Figure 5 Transient experimental and numerical toe length results of the base case

Fig 4 presents the concentration colour maps of the base case, showing the intrusion of the saltwater wedges at the various steady state conditions observed in the experiment. The horizontal extent of the saltwater wedge was 8.8 cm in the physical model, at the end of the first time period. The end of time period 1 will hereafter be regarded as the zero time because the hydraulic gradient in time periods 1 and 3 was the same and results showed no difference in the length of the wedge between both time periods. Therefore, figures showing the transient *TL* will present only time period 2 (advancing wedge; *dh*=4mm) and time period 3 (receding wedge; *dh*=6mm).

The transient experimental and numerical *TL* data are presented in Fig 5. The numerical model matched well the experimental data and was able to reproduce the movement of the toe for the two hydraulic gradients considered. After reducing the head difference to *dh*= 4mm, the saltwater *TL* extended to 17.9 cm and 18.41 cm in the experimental and numerical, respectively. At time t=50 min, the head difference was increased to *dh*=6mm which forced the wedge to retreat back to its original position. The agreement between the experimental and numerical results was generally good. The shape of the saltwater wedge (transition zone and *TL*) at the end of the receding phase was identical to that of the initial condition, indicating that no hysteresis occurred throughout the experiment.

Fig 5 not only shows the reliability of the numerical model for the simulation of the remaining experiments, but it also demonstrates the accuracy of the recorded *TL* data used as baseline for estimating the performance of the barriers The two TL_0 values used for the calculation of R were therefore 8.8 cm and 17.9 cm. These were assumed to be the two extreme saltwater intrusion scenarios for the coastal aquifer system considered.

4.2 Subsurface dam case

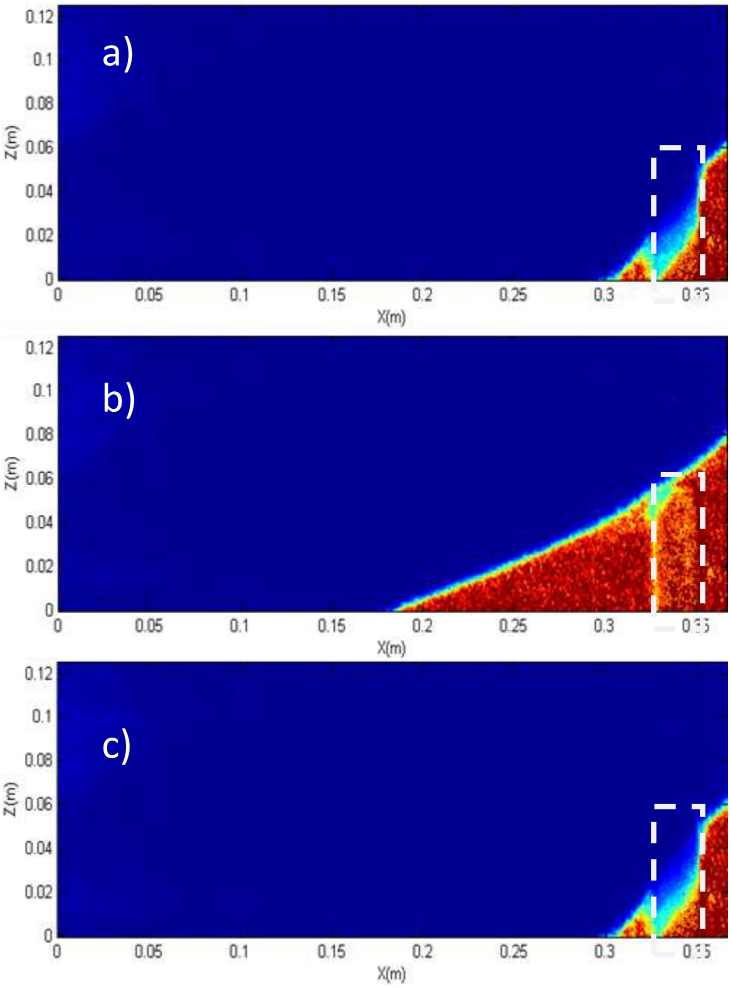

Figure 6 Experimental steady-state saltwater wedge in the subsurface dam case; a) t = 0 min (initial condition); b) at t = 50 min (*dh*=4mm); c) at t = 100 min (*dh*=6mm)

Fig 6 presents the experimental results of the steady state saltwater wedge for different hydraulic gradients. Upon setting the initial condition with *dh*=6mm, the saltwater wedge slowly penetrated into the system until the *TL* reached 7 cm at steady state (Fig 6a). Following the application of head difference *dh*=4mm, the intrusion length extended to 18.8 cm at steady state condition, which corresponds to a percentage of reduction R of -5 %. This negative reduction indicates that the *TL* exceeded that of the baseline case. Laboratory observations revealed that this extension was rather slow and occurred after the dam was almost fully saturated by the saline water (Fig 6b). As the saltwater supply into the system was partially disrupted by the semi-permeable dam, density difference effects caused the saline water in the landward side of the dam to gently slide under the freshwater flow, thereby causing a slight extension of the toe length. Similar observations were reported in Luyun et al. (2009).

After the head difference was reversed to *dh*=6mm at t=50 min, the TL retreated and measured 7 cm at steady state, which corresponds to a percentage reduction R of 21%. This result indicates that the semi-permeable dam could achieve noticeable reduction of the intrusion length only when the hydraulic gradient is high enough to produce sufficient advective forces to help maintain the saltwater wedge on the seaward side of the dam.

The final shape of the wedge was nearly identical to that of the initial condition, suggesting that no hysteresis occurred over the course of the experiment (Fig 6a, 6c). The retreat of the wedge was associated again with a noticeable widening of the transition zone as the interface crosses the semi-permeable dam (Fig 6c). This can be clearly observed in Fig 7 that shows the transient receding wedge after *dh*=6mm was applied to the system. The penetration of the wedge through the dam induced a substantial widening of the transition zone. The low permeability material of the dam primarily slows the movement of the wedge and decreases the freshwater flow velocity. The widening of the transition zone occurring in such conditions is expected to be the result of enhanced separation of streamlines of the freshwater–saltwater mixture induced by flow refraction within the low permeability material of the dam (Lu et al, 2013).

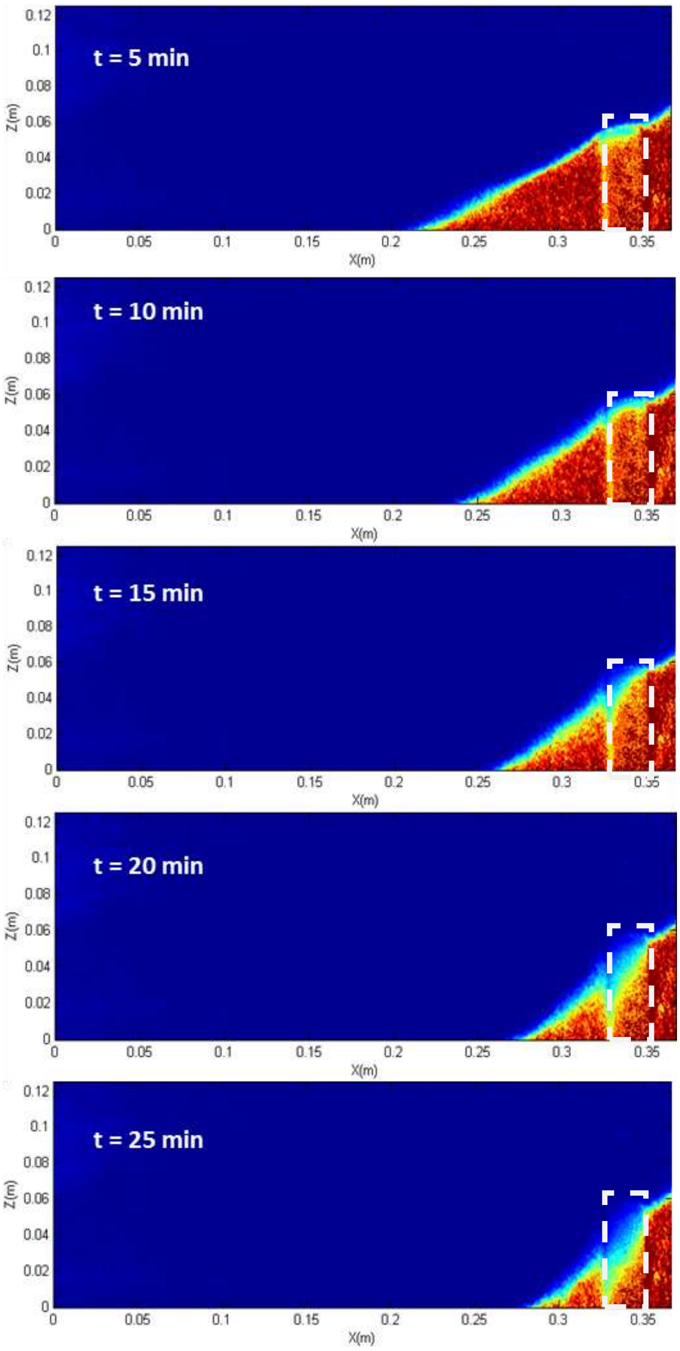

Figure 7 Transient experimental receding saltwater wedge in the subsurface dam case

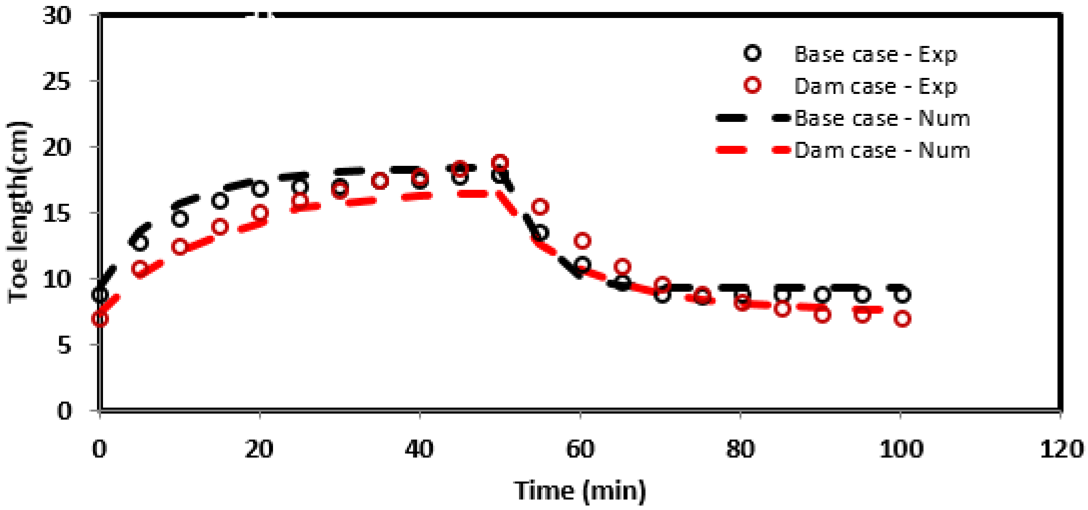

Figure 8 Transient experimental and numerical toe length results of the subsurface dam case

The transient dynamics of the saltwater wedge compared to the numerical prediction is presented in Fig 8 for both the dam and baseline cases. The numerical model reasonably replicated the transient changes of the toe position in the presence of the subsurface dam, for both hydraulic gradients. Smaller values of the *TL* were recorded in the dam case until t=30 min in the experimental model, which suggests that the presence of the subsurface dam temporarily slowed down the rate of the intrusion at the start after which the wedge was forced to flow through the lower permeability material due to the build-up of the saline water pressure behind the dam.

The larger *TL* values observed in the subsurface dam case until t=75-80 min in both the experimental and numerical model suggest that the dam temporarily slowed the natural retreat of saltwater wedge following the increment of the head difference to *dh*=6mm (t=50-100 min). This observation indicates that initially the presence of the low permeability material partially prevented the increased freshwater flow from effectively repulsing the saline water towards the boundary, after which the *TL* values became smaller than the base case. In overall, the results suggest that the use of subsurface dam constructed from semi-permeable materials may not be an effective countermeasure for seawater intrusion control purposes.

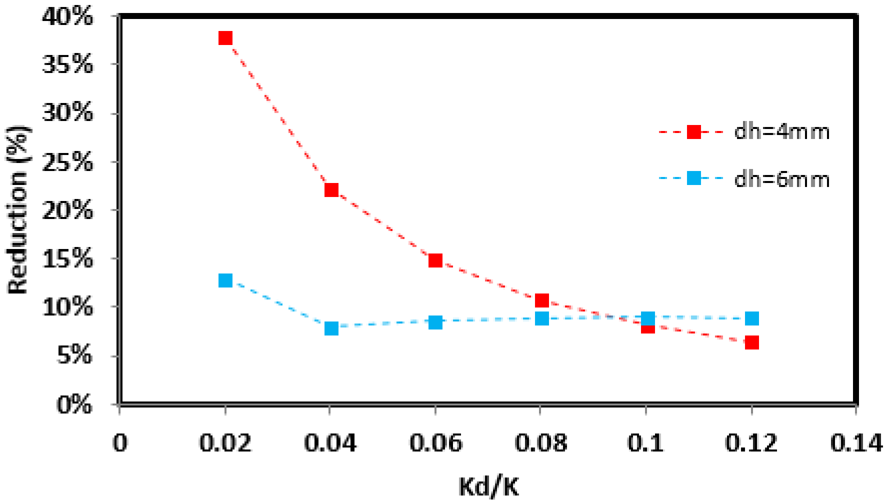

Figure 9 Sensitivity analysis of the effectiveness of the subsurface dam to the permeability ratio K_d/K

Sensitivity analysis was conducted to investigate the effect of the height of the dam and its hydraulic conductivity on the intrusion length. The hydraulic conductivity of the dam was expressed relative to that of the aquifer K_d/K and ranged between 0.02 – 0.12. The dam permeability had small effect on the *TL* for the steeper hydraulic gradient when *dh*=6mm (Fig 9). This is attributed to the greater freshwater flow that repulses the wedge and forces it to remain on the seaward side of the wall anyway. Hence, changing the dam permeability yields little effect in the saltwater wedge reduction. By contrast, the effect of the dam permeability was greater for the smaller head difference *dh*=4mm as the *TL* reduction ranged from R=9% at K_d/K=0.12 to R=38% at K_d/K=0.02. For this hydraulic gradient, the freshwater is unable to build great pressure that halts the wedge and hence in this case the dam is the primary obstacle in the way of the intruding saltwater wedge. Reducing the dam permeability in such case helps in impeding the wedge and thus yields noticeable *TL* reduction. As the hydraulic gradients in real field sites are sometimes lower than the smaller hydraulic gradient investigated here for *dh*=4mm (i=0.0105) particularly at dry seasons, this means that a dam with smaller permeability or impermeable material is an effective tool to repulse the saltwater intrusion especially under such hydrological field conditions with shallow hydraulic gradient.

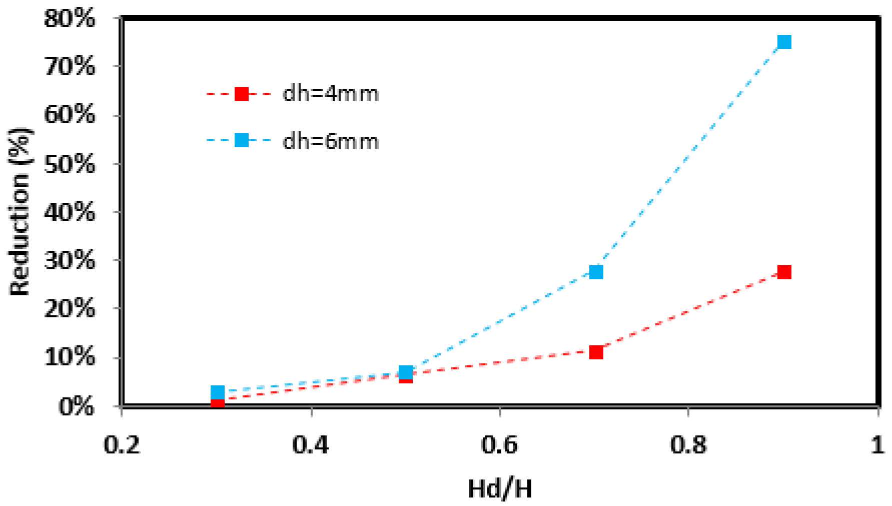

Figure 10 Sensitivity analysis of the effectiveness of the subsurface dam to the ratio H_d/H

The height of the dam was expressed relative to the depth of the aquifer H_d/H and was examined for a range 0.3 - 0.9 (Fig 10). The reduction values ranged from 1% to 28% for *dh*=4mm and between 3% and 75% for *dh*=6mm as H_d/H was varied from 0.3 to 0.9, respectively. The effect of the H_d/H ratio was pronounced in the steeper hydraulic gradient and had insignificant effect in case of *dh*=4mm. Again, this can be attributed to the insufficient freshwater pressure build-up in case of smaller head difference *dh*=4mm to a level that makes the subsurface dam alone unable to significantly prevent the saltwater from further intrusion, regardless of how much the semi-permeable dam covers the aquifer thickness.

4.3 Cutoff wall case

Fig 11 presents the experimental saltwater wedge for the various hydraulic gradients for the cutoff wall case. The first steady state (dh=6mm) was considered as the initial condition (Fig 11a), where the recorded toe was about 4.5 cm from the coastal boundary. Following the application of dh=4mm, the TL extended to 6.7 cm, which corresponds to reduction in the intrusion length of R= 63 % compared to the base case (Fig 11b). Laboratory observations revealed that upon lowering the hydraulic gradient, the saltwater wedge rapidly migrated inland before it promptly stopped at the wall opening. The substantial reduction achieved by the cutoff wall results from the increased freshwater velocity as it flows through the reduced cross section below the wall, thereby effectively repulsing the saline water and forcing it to remain in the seaward side of the wall (Anwar, 1983; Kaleris and Ziogas, 2013; Luyun et al., 2011).

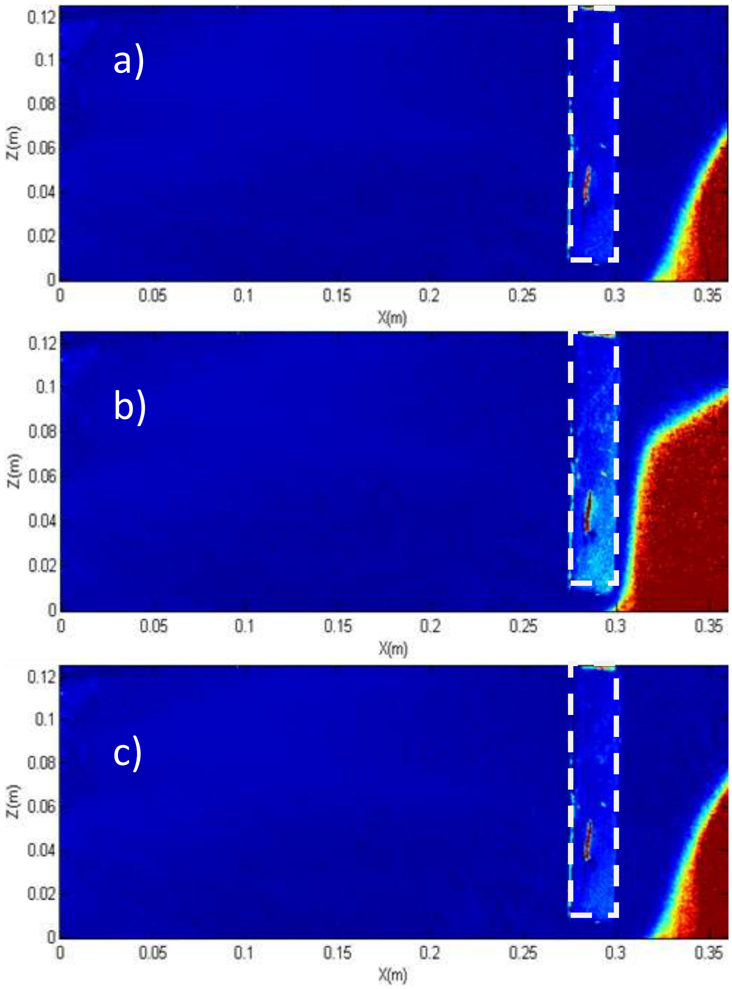

Figure 11 Steady-state experimental saltwater wedge for the cutoff wall case; a) t = 0 min (initial condition); b) at t = 50 min; c) at t = 100 min

After increasing the head difference to *dh*=6mm at t=50 min, the saltwater wedge receded toward the coastal boundary and the *TL* was 4.5 cm at steady state, similar to the observed *TL* at the initial condition (Fig 11c). This corresponds to a toe length reduction of 48% relative to the base case. Laboratory observations reveals that the saltwater retreat was associated with a distortion of the saltwater wedge (t=2.5 min) and a widening of the transition zone (t=5 and 7.5 min), as shown in Fig 12. This interesting observation may be the result of instantaneous increase of the hydraulic gradient which caused an increase of the freshwater flow transmitted to the system. The velocity of freshwater flow was sharply increased at the reduced cross section below the wall, thereby inducing a rather abrupt repulsion of the saltwater wedge associated with a substantial increase of the interface thickness. Such widening of the transition zone was also observed in Robinson et al. (2016) who attributed this to excessive dispersion occurring along the interface essentially induced by the unidirectional flow field that is typically associated with saltwater water retreat (Chang and Clement, 2012).

Numerical results of the transient toe length for the cutoff wall case are well matched with the experimental data (Fig 13). The system rapidly reached a state of equilibrium within 10 minutes for both hydraulic gradients. The reduction achieved by the cutoff wall was significantly greater for the lower hydraulic gradient. Regardless of the extent of the saltwater wedge before the barrier installation, the cutoff wall was able to maintain the wedge on the seaward side for all the hydraulic gradients tested. Hence the reduction is higher for the smaller hydraulic gradient which initially induced greater *TL* before the wall installation. This shows the long term reliability of cutoff walls in effectively reducing saltwater intrusion, where the reduction is more pronounced in smaller or shallower hydraulic gradients than steeper gradients. This result demonstrates that the worthiness of installing cutoff walls for seawater intrusion control purposes increases in shallower hydraulic gradients.

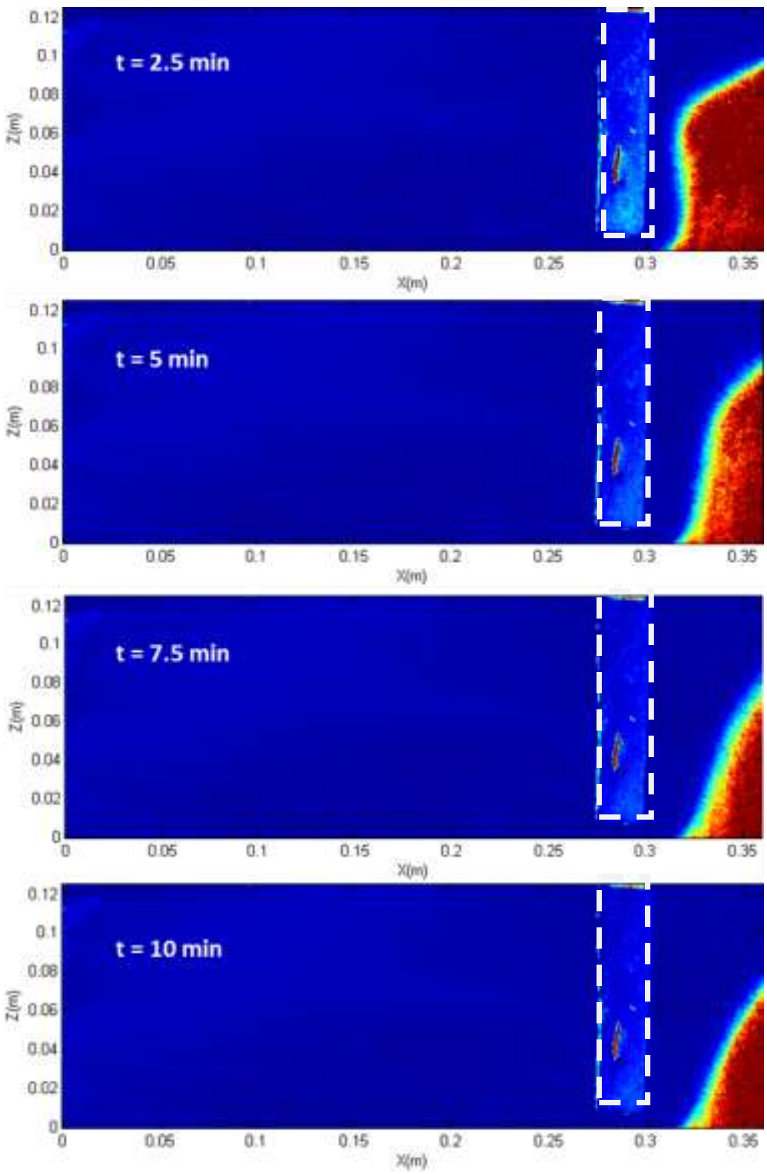

Figure 12 Transient experimental receding saltwater wedge for the cutoff wall case

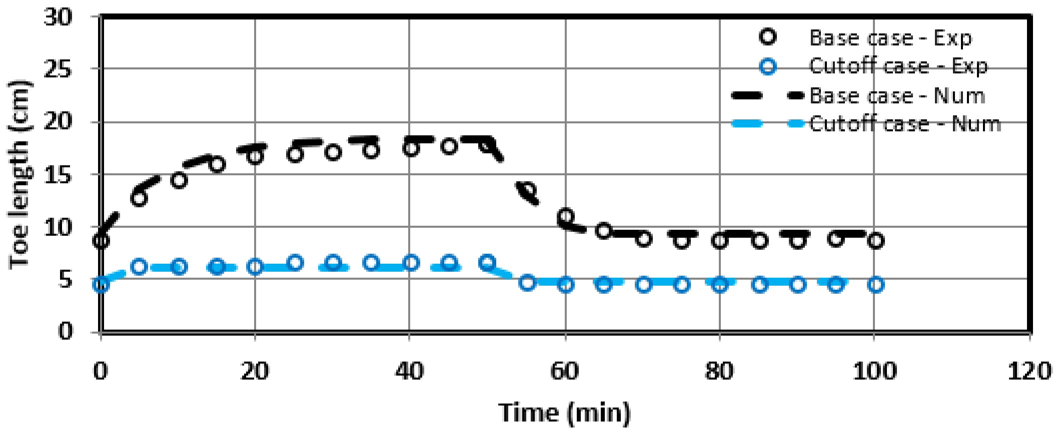

Figure 13 Transient experimental and numerical toe length results of the cutoff wall case

4.4 MPB case

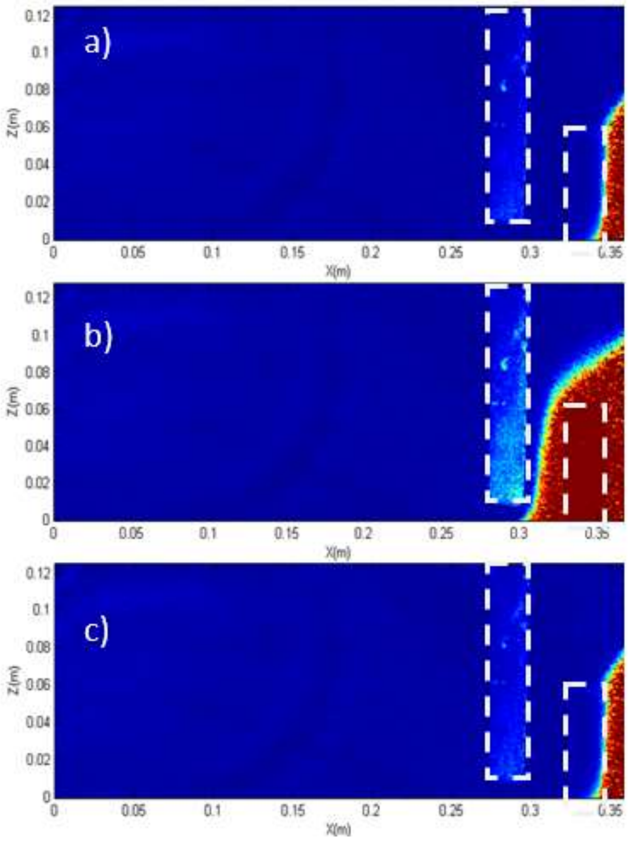

Figure 14 Steady-state experimental saltwater wedge in the MPB case; a) t = 0 min (initial condition); b) at t = 50 min; c) at t = 100 min

Fig 14 presents the experimental steady state saltwater wedges for the MPB case. The design parameters of the cutoff wall and the dam cases used here are the same as in the cutoff wall case and subsurface dam case, respectively. Upon imposing the first boundary conditions (*dh*=6mm), the saline water intruded the system before it was abruptly stopped at the position of the subsurface dam (Fig 14a). The initial intrusion length was 2.6 cm, compared to *TL*=8.8 cm recorded in the base case. It is interesting to note that unlike the subsurface dam case, the saline water did not penetrate through the dam here.

After applying a head difference of *dh*=4mm, the saltwater completely penetrated through the dam. The steady state *TL* was 6.9 cm, corresponding to a reduction R of 61% (Fig 14b). This result indicates that when the freshwater flow was not sufficiently high to prevent the complete saturation of the dam by the saline water, the MBP exhibited similar performance as the single cutoff wall. Laboratory observations revealed the existence of a saltwater lifting mechanism, whereby the residual saline flux was gradually lifted upward and transported over the dam toward the outlet (Fig 15a). This lifting also occurred over the course of the receding phase after increasing the head difference to *dh*=6mm (Fig 15b). To the best of our knowledge, this lifting mechanism has not been observed by previous studies. The images clearly show the freshwater flowing through the semi-permeable material of the dam and transporting the dense saline water along the interface.

The performance of cutoff walls located nearby the coastline (less than half of the aquifer thickness) depends on the velocity ratio of the freshwater inflow velocity over the velocity of the intruding saltwater driven by density differences (Kaleris and Ziogas, 2013). The combined effects of the cutoff wall and the semi-permeable dam induces an increase of the velocity ratio within the spacing between the barriers, which imposes more resistance to density contrast effects and allows the light freshwater to lift the denser liquid and discharge it outside the domain thereby ensuring an effective obstruction of the saltwater wedge on the seaward side of the dam. The recorded *TL* was 2.6 cm when the system reached final steady state, which corresponds to a reduction of 70% of the intrusion length (Fig 14c). In other words, the MPB achieved up to 62% and 42% more intrusion length reduction compared to the toe length recorded in the subsurface dam and the cutoff wall cases, respectively.

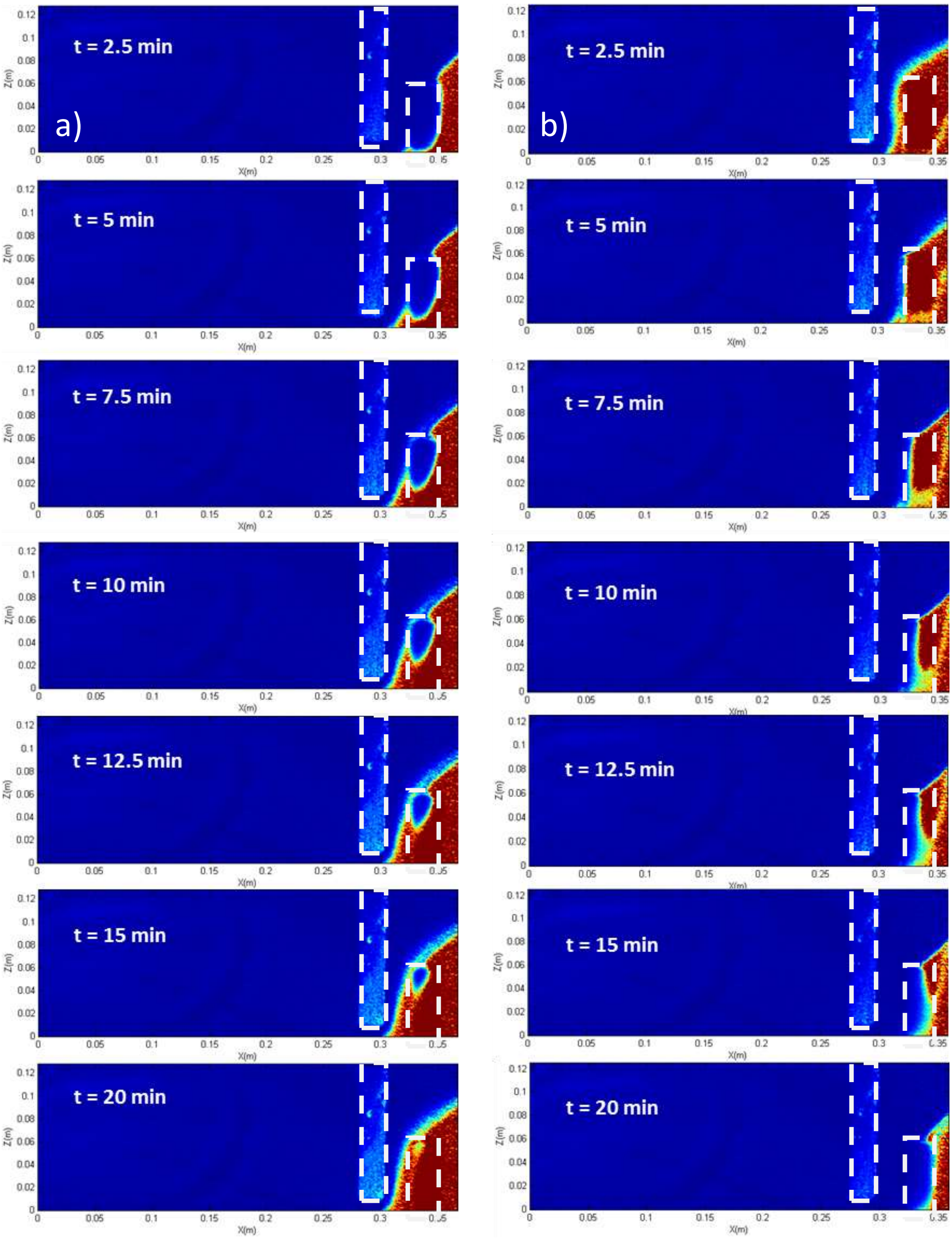

Figure 15 Experimental images of the saltwater lifting mechanism a) intruding condition (*dh*=4mm) b) receding condition (*dh*=6mm)

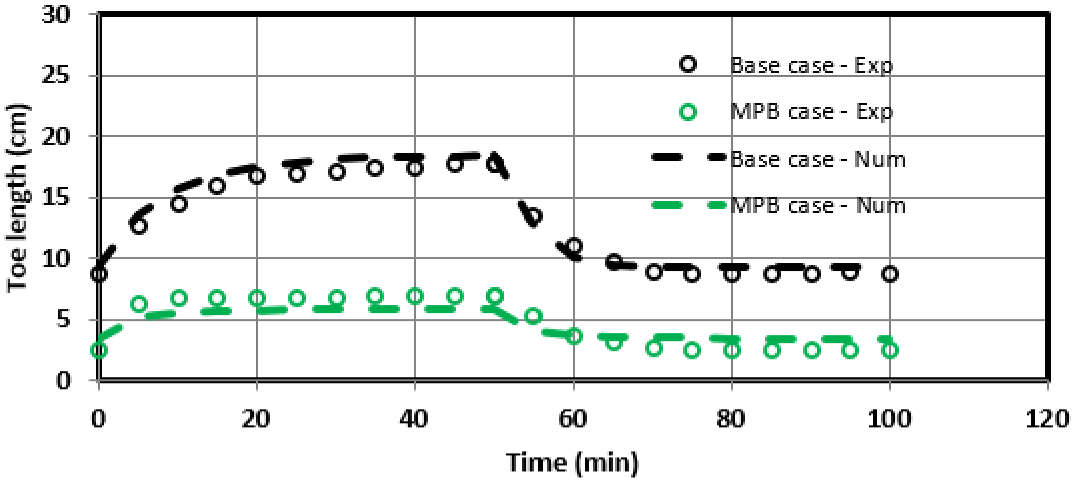

Figure 16 Transient experimental and numerical toe length results of the MPB case

The transient dynamics of the saltwater wedge are shown in Fig 16. The transient toe movement was well reproduced by the numerical model for both hydraulic gradients. The experimental and numerical data show that the system reached steady state within 15min for both hydraulic gradients. Additional simulations were conducted to investigate the influence of various key parameters on the saltwater intrusion length in presence of the MPB. The simulations were run solely for *dh*=6mm where the MPB exhibited the highest efficiency. Simulations were also run for single cutoff wall for the purpose of comparison. The *TL* was measured to characterize the effectiveness of the two barriers relative to each other. The MPB was found considerably more effective than the subsurface dam, even when the latter was impervious, and hence for this reason, the case of single semi-permeable dam was not included in the sensitivity analysis.

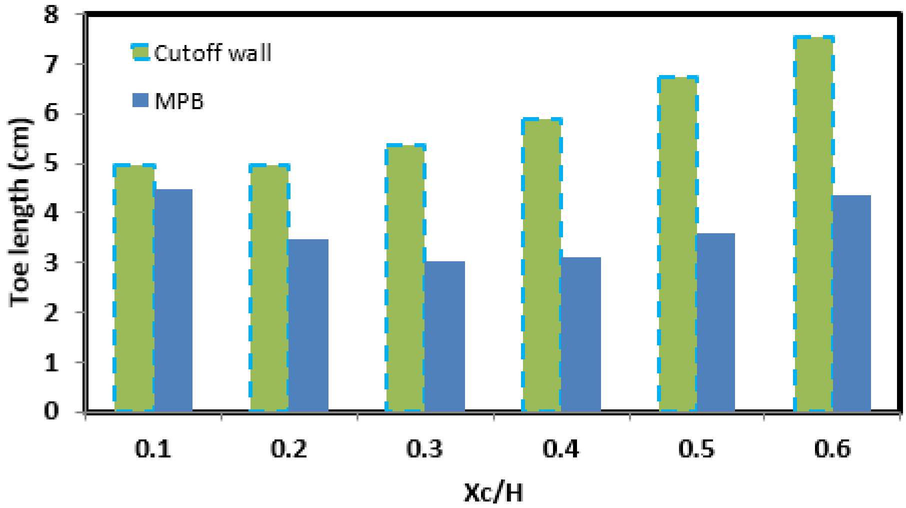

Figure 17 Effect of the ratio X_c/H on the intrusion length in presence of the MPB

The effect of the wall opening size (distance between the wall and aquifer bed) was first examined, where six X_c/H ratios over the range 0.1-0.6 were tested. Fig 17 shows the *TL* results in presence of a MPB and a single cutoff wall. The MPB induced 10% (X_c/H =0.1) and 42% (X_c/H=0.6) more reduction in the intrusion length than the cutoff wall. The smallest intrusion length was observed for X_c/H=0.3 in the MPB case. The results indicate that the effect of MPB on the intrusion length is greater than that of the single cutoff as the wall opening size is increased. The MPB remains very effective up to opening size as large as X_c/H=0.6, which may imply considerable construction cost saving. In addition, the 42% extra reduction introduced by the MPB system for X_c/H=0.6 could not be achieved when using single cutoff wall even for wall penetration depth covering 90% of the aquifer thickness (X_c/H=0.1). In such scenario, the MPB was not only substantially more effective in controlling the intrusion, but could also induce considerable construction cost savings, depending on the site specific hydrogeological conditions. This may be of particular importance for deep aquifers where the difference in the penetration depth between the MPB and the cutoff wall may induce significant saving, even considering the need to construct semi-permeable dam in the MPB case.

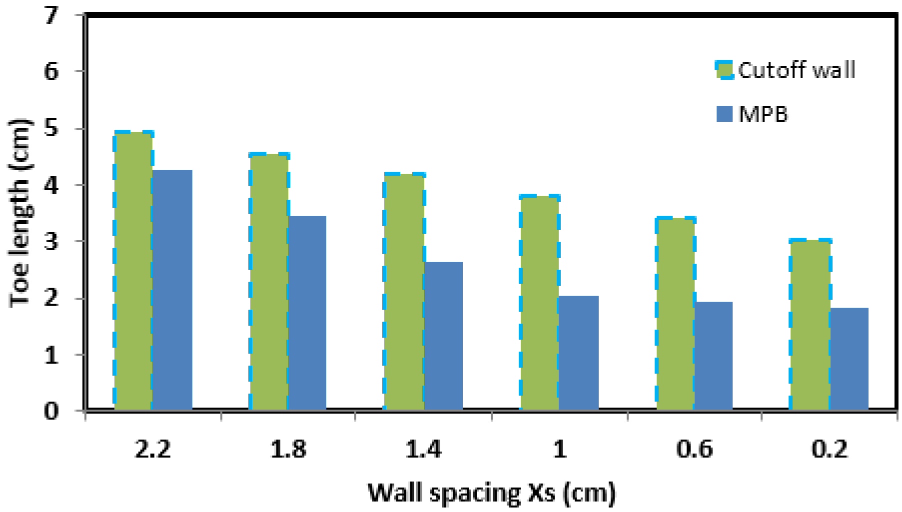

Figure 18 Effect of the spacing Xs on the intrusion length in presence of the MPB

The effect of the spacing X_s between the cutoff and the dam was also investigated. The subsurface dam was maintained at the same position, while the cutoff was moved seaward, such that six values of X_s ranging between 0.2-2.2 cm were investigated (Fig 18). The reduction of the *TL* achieved by the MPB increased by decreasing the spacing X_s, with a more pronounced reduction than a single cutoff. The smallest intrusion length was recorded at X_s=0.2 cm in the MPB case, albeit this may be hardly feasible in practical situation. Note that for the range 0.2-1.0 cm, only little effect on the toe length was observed in the case of the MPB, while the performance of the single cutoff wall reached a maximum value for a wall position corresponding to X_s=0.2 cm, i.e. when the wall was installed at 4.6 cm from the coastline boundary. The *TL* was 1.82 cm and 3.02 cm for the MPB and single cutoff, respectively. In other words, the MPB achieved 40% more saltwater wedge reduction than the single cutoff for the smallest spacing considered. Given that moving the cutoff in the seaward direction would allow greater fresh groundwater storage, this finding implies that a more optimal use of the available freshwater could be associated with a more effective control of the saltwater intrusion process using an MPB system compared to a single cutoff wall system, for equivalent seaward displacement of the impermeable wall.

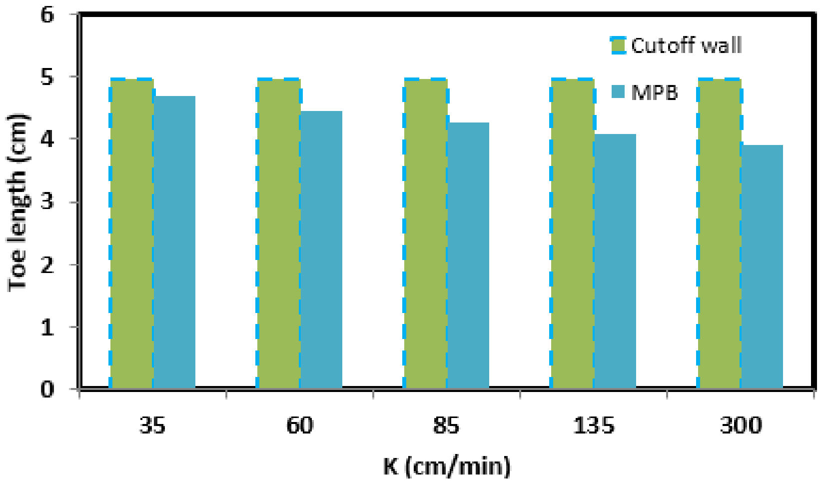

Figure 19 Effect of the aquifer hydraulic conductivity on the intrusion length in presence of the MPB

The effect of the hydraulic conductivity of the porous medium on the barrier performance was examined over the range 35-300 cm/min (Fig 19). While the *TL* remains nearly the same in presence of single cutoff wall for the various K values, it continuously decreases with increasing K when using the MPB barrier system. The effect of hydraulic conductivity in the MPB case may be attributed to the permeability contrast between the dam and the background aquifer permeability, which keeps varying for different aquifer permeability. As the latter increases, this contrast ratio becomes bigger. The MPB induced between 5% and 21% more reduction than the cutoff wall as K varied from 35 to 300 cm/min respectively. This result indicates that the relative effectiveness of MPB compared to a single cutoff is expected to increase with increasing aquifer hydraulic conductivity.

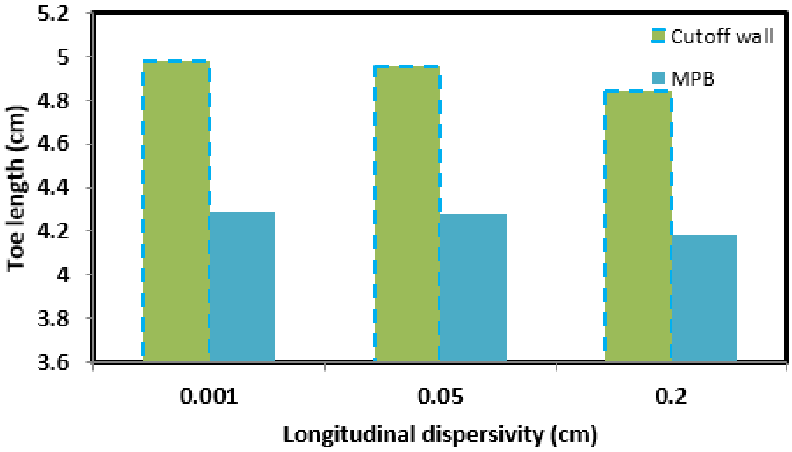

Figure 20 Effect of the longitudinal dispersivity of the aquifer on the intrusion length in presence of the MPB

The effect of the dispersivity coefficients on the performance of MPB was also investigated (Fig 20). Three values of longitudinal dispersivity were tested: 0.001, 0.05 and 0.2 cm. The transversal to longitudinal dispersivity ratio remained constant. The net *TL* reduction was estimated at 2.5% and 2.8%, for the MPB and the cutoff wall, respectively. For the lowest and highest dispersivity values considered, the MPB induced about 14% additional reduction in the *TL* for the two extreme dispersivity values considered. The results show that the effectiveness of the MPB increases for systems with higher dispersivity. The impact of MPB on the saltwater intrusion length compared to that of a single cutoff wall is therefore expected to be greater in highly dispersive coastal groundwater systems.

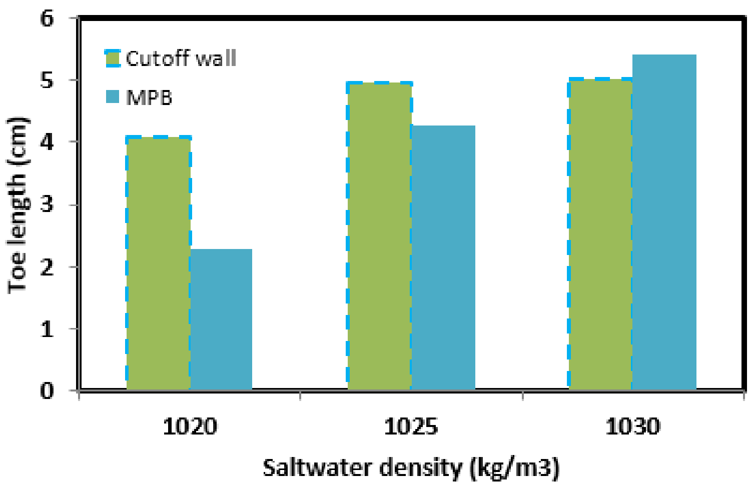

Figure 21 Effect of the saltwater density on the intrusion length in presence of the MPB

Results of the influence of the density contrast on *TL* are presented in Fig 21, where three saltwater density contrast between seawater and freshwater of 1.020, 1.025 and 1.030 were examined. The increase in density contrast induced an increase of the intrusion length by 57% for the MPB case, and 18% for the single cutoff case. For the lowest density, the MPB achieved 44% more reduction than the single cutoff wall. By contrast, for the highest density difference considered, the single cutoff achieved about 7.8% more reduction of the *TL* than the MPB. The results show that the effectiveness of the MPB increases substantially for lower saltwater density. Obviously, the decrement of the saltwater density eases the lifting of saline flux by the MPB. This result implies that the MPB may display good efficiency in real scale aquifer setting, particularly in zones where wide transition zone generally occurs, where saltwater concentration is subsequently reduced as a result of micro/macro scale heterogeneity. The results suggest that more reduction of the intrusion length may be achieved with the MPB than a single cutoff in coastal groundwater systems with saltwater solutions inferior or equal to 1025 kg/m^3. The performance of the MPB may however be lower for higher saltwater density values.

5. Summary and Conclusions

This study provides a thorough analysis of the effect of subsurface physical barriers on saltwater intrusion dynamics under transient conditions. A new barrier system was suggested as saltwater intrusion control method: the mixed physical barrier MPB, which combines an impermeable cutoff wall and semi-permeable subsurface dam located on its seaward side. Using laboratory experiments and numerical simulations, the effect of the semi-permeable subsurface dam, cutoff wall and MPB on saltwater intrusion dynamics was investigated for different hydraulic gradients. The sensitivity of the performance of these different barriers to some key design and hydrogeological parameters was then explored. The main findings of the study are:

- Subsurface dams constructed from semi-permeable material do not provide suitable control of the saltwater intrusion process. A reduction in the toe length may be exhibited provided that the groundwater flux is sufficiently high to assist dam in retaining the intruding saltwater wedge. They primarily affect the rate of the saltwater transport process but this effect is rapidly dissipated after complete saturation of the dam by the saline water. In the cases investigated here, the semi-permeable dam eventually induced a negative effect on wedge length when the hydraulic gradient was lower, causing the toe length to extend beyond the toe location observed prior the dam installation.
- The worthiness of installing cutoff walls for saltwater intrusion control purposes increases as the hydraulic gradient becomes smaller or shallower. In the cases considered here, the cutoff wall was able to reduce the toe length by up to 63%.
- The MPB induced a visible saltwater lifting process, whereby freshwater flowing below the wall opening with increased velocity transported dispersive flux of saltwater above the subsurface dam and discharged it towards the outlet. This lifting mechanism has significant effect on the intrusion length, especially when the hydraulic gradient was relatively steep, where it yielded up to 70% reduction of the initial intrusion length, corresponding to 42% more reduction than the single cutoff wall and 62% more than the semi permeable subsurface dam alone.
- While the effectiveness of single cutoff walls is limited to wall opening sizes not exceeding 40% of the aquifer thickness, the MPB exhibited good reduction for wall opening size extending up to 60% of the aquifer thickness, where it could exhibit up to 42% more reduction than a single cutoff wall. This reduction could not be achieved using single cutoff wall even for wall penetration depth covering 90% of the aquifer thickness. This finding therefore implies that there may be a potential for construction cost savings by installing impermeable wall with shorter penetration depth when using MPB (especially in deep

coastal aquifer systems), and at the same time best ensuring the repulsion of intruding saline water.

- For equivalent seaward displacement of the impermeable wall, the MPB displayed better obstruction of the intruding saline water, achieving up to 40% more intrusion length reduction than the single cutoff wall. This finding implies that displacing the impermeable wall of the MPB seaward would not only ensure a more reliable prevention against saltwater intrusion, but also allow a more optimal use of the available freshwater volume, which is essential from a prospective of water resources management.
- The effectiveness of the MPB was found to increase with increasing hydraulic conductivity, dispersivity and decreasing saltwater density (<1025 kg/m3) of the coastal groundwater system.

In field applications, the installation of the MPB is expected to be more suitable in high hydraulic conductivity aquifers (e.g. sand, gravel), where the groundwater flow velocity is high. In such conditions, the effect of the MPB in increasing the freshwater inflow velocity over the velocity of the intruding saltwater within the spacing between the wall and the semi-permeable dam will be more feasible. In addition, real aquifers generally exhibit higher dispersion often associated with micro/macro scale heterogeneity, which results in considerable widening of the freshwater-saltwater transition zone with different salt concentrations. Consequently, the toe of a marine saltwater intrusion may meet the inland freshwater with only slightly elevated concentrations (brines). This low density contrast between the intruding saline water and fresh groundwater may therefore further enhance the ability of the MPB to lift up saline flux and repulse it seaward.

Additional experiments and modelling would however be recommended for future work to further explore the field practicability of this system. For instance, the effect of large-scale model, 3D effects and the bottom boundary morphology are clearly worthy of further analyses.

Our ongoing work focus on this and also on exploring the effectiveness of the MPB in heterogeneous aquifers and this shall be the subjects of future publications.

Acknowledgements

The authors wish to thank Queen’s University Belfast for supporting the research project by the mean of a PhD studentship accorded to the first author. Thanks to Gareth Robinson for his introductory training to the experimental methodology employed in this study. Thanks also go to Paul Lamont-Kane for providing valuable comments.

References

Abarca, E., Carrera, J., Sánchez-Vila, X., Dentz, M., 2007. Anisotropic dispersive Henry problem. Adv.Water Resour. 30, 913-926.

Abarca, E., Clement, T.P., 2009. A novel approach for characterizing the mixing zone of a saltwater wedge. Geophys.Res.Lett. 36, L06402.

Abarca, E., Vázquez-Suñé, E., Carrera, J., Capino, B., Gámez, D., Batlle, F., 2006. Optimal design of measures to correct seawater intrusion. Water Resour.Res. 42, DOI: 10.1029/2005WR004524.

Allow, K.A., 2012. The use of injection wells and a subsurface barrier in the prevention of seawater intrusion: a modelling approach. Arabian J Geosci. 5, 1151-1161.

Anwar, H., 1983. The effect of a subsurface barrier on the conservation of freshwater in coastal aquifers. Water Res. 17, 1257-1265.

Archwichai, L., Mantapan, K., & Srisuk, K., 2005. Approachability of subsurface dams in the Northeast Thailand. In International conference on geology, geotechnology and mineral resources of Indochina . 28-30.

Basdurak, N. B., Onder, H., & Motz, L. H. 2007. Analysis of Techniques to Limit Saltwater Intrusion in Coastal Aquifers. In World Environmental and Water Resources Congress 2007: Restoring Our Natural Habitat. 1-8.

Bear, J., 1979. Groundwater hydraulics. McGraw, New York.

Bear, J., Cheng, A.H.D., Sorek, S., Ouazar, D. and Herrera, I. eds., 1999. Seawater intrusion in coastal aquifers: concepts, methods and practices. Springer Science & Business Media.

Botero-Acosta, A., Donado, L.D., 2015. Laboratory Scale Simulation of Hydraulic Barriers to Seawater Intrusion in Confined Coastal Aquifers Considering the Effects of Stratification. Procedia Environ Sci. 25, 36-43.

Chang, S.W., Clement, T.P., 2013. Laboratory and numerical investigation of transport processes occurring above and within a saltwater wedge. J.Contam.Hydrol. 147, 14-24.

Chang, S.W., Clement, T.P., 2012. Experimental and numerical investigation of saltwater intrusion dynamics in flux-controlled groundwater systems. Water Resour.Res. 48, W09527.

Ferguson, G., Gleeson, T., 2012. Vulnerability of coastal aquifers to groundwater use and climate change. Nat Clim Change. 2, 342-345.

Goswami, R.R., Clement, T.P., 2007. Laboratory-scale investigation of saltwater intrusion dynamics. Water Resour.Res. 43, W04418.

Guo, W., Langevin, C.D., 2002. User's guide to SEAWAT; a computer program for simulation of three-dimensional variable-density ground-water flow.

Japan Green Resources Agency, 2004. Technical Reference for Effective Groundwater Development.

Johannsen, K., Kinzelbach, W., Oswald, S., Wittum, G., 2002. The saltpool benchmark problem–numerical simulation of saltwater upconing in a porous medium. Adv.Water Resour. 25, 335-348.

Kaleris, V.K., Ziogas, A.I., 2013. The effect of cutoff walls on saltwater intrusion and groundwater extraction in coastal aquifers. J Hydrol. 476, 370-383.

Kumar, C.P., 2006. Management of groundwater in salt water ingress coastal aquifers. Groundwater Modelling and Management. 540-560.

Lu, C., Chen, Y., Zhang, C., Luo, J., 2013. Steady-state freshwater–seawater mixing zone in stratified coastal aquifers. J Hydrol. 505, 24-34.

Luyun Jr., R., Momii, K., Nakagawa, K., 2009. Laboratory-scale saltwater behavior due to subsurface cutoff wall. J Hydrol. 377, 227-236.

Luyun, R., Momii, K., Nakagawa, K., 2011. Effects of recharge wells and flow barriers on seawater intrusion. Ground Water. 49, 239-249.

Oostrom, M., Hayworth, J.S., Dane, J.H., Güven, O., 1992. Behavior of dense aqueous phase leachate plumes in homogeneous porous media. Water Resour.Res. 28, 2123-2134.

Oude Essink, G.H.P., 2001. Improving fresh groundwater supply—problems and solutions. Ocean Coast.Manage. 44, 429-449.

Pool, M., Carrera, J., 2010. Dynamics of negative hydraulic barriers to prevent seawater intrusion. Hydrogeol.J. 18, 95-105.

Robinson, G., Ahmed, A.A., Hamill, G.A., 2016. Experimental saltwater intrusion in coastal aquifers using automated image analysis: Applications to homogeneous aquifers. J Hydrol. 538, 304-313.

Robinson, G., Hamill, G.A., Ahmed, A.A., 2015. Automated image analysis for experimental investigations of salt water intrusion in coastal aquifers. J Hydrol. 530, 350-360.

Sriapai, T., Walsri, C., Phueakphum, D., Fuenkajorn, K., 2012. Physical model simulations of seawater intrusion in unconfined aquifer. Songklanakarin J Sci Technol. 34, 679-687.

Sugio, S., Nakada, K., Urish, D.W., 1987. Subsurface seawater intrusion barrier analysis. J.Hydraul.Eng. 113, 767-779.

Voss, C.I., Souza, W.R., 1987. Variable density flow and solute transport simulation of regional aquifers containing a narrow freshwater- saltwater transition zone. Water Resour.Res. 23, 1851-1866.